Xanthomonas translucens commandeers the host rate-limiting step in ABA biosynthesis for disease susceptibility

Zhao Peng[a,1], Ying Hu[b,2], Junli Zhang[a,3], Jose C. Huguet-Tapia[a], Anna K. Block[c], Sunghun Park[d], Suraj Sapkota[e,4], Zhaohui Liu[e], Sanzhen Liu[b], and Frank F. White[a,1]

[a]Department of Plant Pathology, University of Florida, Gainesville, FL 32611; [b]Department of Plant Pathology, Kansas State University, Manhattan, KS 66506; [c]Center for Medical, Agricultural, and Veterinary Entomology, US Department of Agriculture-Agricultural Research Service, Gainesville, FL 32608; [d]Department of Horticulture and Natural Resources, Kansas State University, Manhattan, KS 66506; and [e]Department of Plant Pathology, North Dakota State University, Fargo, ND 58108

Edited by Sean R. Cutler, University of California, Riverside, CA, and approved September 13, 2019 (received for review July 8, 2019)

Plants are vulnerable to disease through pathogen manipulation of phytohormone levels, which otherwise regulate development, abiotic, and biotic responses. Here, we show that the wheat pathogen *Xanthomonas translucens* pv. *undulosa* elevates expression of the host gene encoding 9-*cis*-epoxycarotenoid dioxygenase (*TaNCED-5BS*), which catalyzes the rate-limiting step in the biosynthesis of the phytohormone abscisic acid and a component of a major abiotic stress-response pathway, to promote disease susceptibility. Gene induction is mediated by a type III transcription activator-like effector. The induction of *TaNCED-5BS* results in elevated abscisic acid levels, reduced host transpiration and water loss, enhanced spread of bacteria in infected leaves, and decreased expression of the central defense gene *TaNPR1*. The results represent an appropriation of host physiology by a bacterial virulence effector.

Xanthomonas | ABA | TAL effector | disease susceptibility | wheat

Plant hormone signaling controls multiple facets of plant responses in development, as well as biotic and abiotic stress, and plants are, therefore, vulnerable to disease by pathogens that can alter phytohormone levels (1, 2). A variety of bacterial plant pathogens synthesize phytohormones during the infection process, including auxin, cytokinin, and gibberellins (3–6). *Agrobacterium tumefaciens* transfers genes for autonomous auxin and cytokinin production to the host genome (7, 8). *Pseudomonas syringae* produces the toxin coronatine, which mimics the phytophormone jasmonic acid (JA) (9). The type III effector AvrRpt2 has been shown to increase host auxin sensitivity through an unknown mechanism of reduction of the auxin response repressors, AXR2 and AXR3 (10). Type III effectors HopZ1 and HopX1 of *P. syringae* activate the JA pathway by bypassing JA itself and inactivating the jasmonate ZIM-domain (JAZ) proteins, which act as repressors of JA-responsive genes (1, 2, 11, 12). Oomycetes, fungi, and bacteria are known to reduce or enhance levels of the drought-responsive phytohormone abscisic acid (ABA) (2, 13). Elevated ABA levels have been both correlated with susceptibility and resistance in filamentous pathogens and, indeed, some fungi synthesize ABA, which may represent a virulence factor (13, 14). In the case of bacteria, several type III virulence effectors are associated with enhanced ABA levels. AvrXccC of *Xanthomonas campestris* pv. *campestris* has been associated with elevated ABA levels in *Arabidopsis* infections (15). Two effectors of *P. syringae* DC3000, AvrPto and AvrPtoB, have been associated with ABA increases, while HopAM1 is associated with inducing hypersensitivity to ABA (16–18). How individual effectors alter ABA sensitivity or levels is unknown.

Some members of the genus *Xanthomonas* deploy a distinct family of type III effectors known as transcription activator-like (TAL) effectors. TAL effectors bind host gene promoters in a sequence-specific manner and add plasticity to adaption of the bacteria to host plants by direct manipulation of host gene expression (19–21). *Xanthomonas translucens* causes disease on a wide variety of grass species, including the subspecies pathovar *X. translucens* pv. *undulosa* (*Xtu*), which is a pathogen of wheat. *Xtu* strains harbor 7 to 8 TAL effector genes (22, 23). Here, we examined the role of TAL effectors in *Xtu* and attempted to identify TAL effector associated susceptibility genes in wheat infections.

Results

Tal8 Is Associated with Enhanced Virulence in XT4699. *Xtu* causes the disease known as bacterial leaf streak of wheat (Fig. 1*A*) and virulence assays were conducted by injection of bacteria into young leaves with a needle-less syringe, which resulted in water-soaked streaked lesions from the inoculation site (Fig. 1*B*). Assays were conducted on mutants for each of 8 TAL effector genes in *Xtu*

Significance

Pathogenic bacteria acquire new virulence strategies for exploiting their hosts. This work reveals that the bacterial wheat pathogen *Xanthomonas translucens* uses a transcription activation-like (TAL) effector to promote virulence by directly activating the host gene 9-*cis*-epoxycarotenoid dioxygenase, the rate-limiting enzyme in biosynthesis of abscisic acid that is normally involved in water management within the host plant. Evolutionarily, TAL effectors are a relatively new class of virulence factors limited to a few species of pathogenic bacteria, and this work adds to the diversity of host susceptibility genes that can be exploited by pathogens through TAL effector gene function.

Author contributions: Z.P., Y.H., A.K.B., S.P., Z.L., S.L., and F.F.W. designed research; Z.P., Y.H., J.Z., J.C.H.-T., A.K.B., S.P., S.S., and S.L. performed research; Z.P., Y.H., J.Z., J.C.H.-T., A.K.B., S.P., S.L., and F.F.W. analyzed data; and Z.P., Z.L., S.L., and F.F.W. wrote the paper.

The authors declare no competing interest.

This article is a PNAS Direct Submission.

Data deposition: RNA sequencing data were deposited in the National Center for Biotechnology Information Sequence Read Archive (SRA) database (accession no. PRJNA485724). Xtu LW16 genome assembly was deposited under GenBank accession no. CP043540.1, https://www.ncbi.nlm.nih.gov/nuccore/CP043540.1/; and P3 genome assembly was deposited under accession no. CP043500, https://www.ncbi.nlm.nih.gov/nuccore/CP043500/.

[1]To whom correspondence may be addressed. Email: zpeng15@ufl.edu or ffwhite@ufl.edu.

[2]Present address: Department of Horticultural Sciences, University of Florida, Gainesville, FL 32611.

[3]Present address: Department of Wildlife Ecology and Conservation, University of Florida, Gainesville, FL 32611.

[4]Present address: Institute of Plant Breeding, Genetics, and Genomics, University of Georgia, Griffin Campus, Griffin, GA 30223.

This article contains supporting information online at www.pnas.org/lookup/suppl/doi:10.1073/pnas.1911660116/-/DCSupplemental.

First published October 1, 2019.

strain XT4699 (strains used in this study are listed in *SI Appendix*, *Supplementary Information Text* and Table S1). Mutant M6, lacking the gene $tal8_{XT4699}$ (hereafter *tal8*) and containing the empty cloning vector (ev), incited shorter lesions in comparison to the WT strain XT4699 in 2 cultivars, the winter wheat cultivar (cv) Jagger (Fig. 1 *B* and *C* and *SI Appendix*, Fig. S1*A*) and the spring wheat cv Chinese Spring (*SI Appendix*, Fig. S1 *B* and *C*). The reintroduction of *tal8* into M6 restored virulence in comparison to M6 (ev) on both cultivars (Fig. 1 *B* and *C* and *SI Appendix*, Fig. S1 *A*–*C*). No differences in total leaf and surface bacterial populations were detected between WT, M6 (ev), and M6 (*tal8*) in either cultivar (*SI Appendix*, Fig. S1 *D* and *E*). However, populations of M6 (ev) were reduced in the section of leaves distal from the inoculation site in comparison to WT and M6 (*tal8*), indicating that more bacteria were distributed farther up and down the leaf in the presence of *tal8* (Fig. 1 *D* and *E*).

***TaNCED* and *TaERF* Are Candidate Host Susceptibility Genes for Tal8.** RNA-sequencing (RNA-seq) expression profiles of infected leaf samples were compared for both Jagger and Chinese Spring wheat cultivars with either WT or mutant bacteria (*SI Appendix*) (24). Candidate disease susceptibility genes corresponding to the effector $Tal8_{XT4699}$ (hereafter Tal8) were selected according to relative fold-change in expression between WT and mutant treatments from the Jagger cultivar (*SI Appendix*). The candidate genes were then ranked by the effector binding element (EBE) prediction score (*SI Appendix*), and the proximity of the EBE to the ATG and the fold-change in Chinese Spring treatment were noted (Table1). The specific EBEs were predicted from the repeat variable di-amino acid residue (RVD) region of the Tal8 protein, treating the unusual RVDs, KG, Y*, and QD as functionally equivalent to NG, N*, and HD of the consensus RVDs (*SI Appendix*, Fig. S2). Among the top ranked genes, 2 homeologous sets of genes were noted. Traes_5BS_B626C522B represents a gene for 9-*cis*-epoxycarotenoid dioxygenase 3 (NCED) located on the short arm of chromosome 5 of the B genome of hexaploid wheat, and was designated *TaNCED_5BS* (Table 1). The promoter region of *TaNCED_5BS* is conserved among the B, A, and D genome copies of the gene, although polymorphisms are present at the EBE region (*SI Appendix*, Fig. S3*A*). Traes_1BL_F0C52C5DF on the long arm of chromosome 1B represents a member of the apetala-2/ethylene response factor (AP-2/ERF) family and was designated *TaERF_1BL* (Table 1). *TaERF_1BL* has homeologs on the A and D genomes, and the predicted EBEs are identical (*SI Appendix*, Fig. S3*B*). The D genome copy of *TaNCED* was also induced as well as *TaERF* homeologs on the A and D genomes (Table 1 and *SI Appendix*, Fig. S3). No evidence was obtained for enhanced expression of *TaNCED_5AS*, which may be due to the TT > GC transversions in the corresponding EBE regions (*SI Appendix*, Fig. S3*A*). The proposed EBE for Tal8 lies 26 bp upstream of the putative TATA box of *TaNCED_5BS* (Fig. 2*A*). No TATA box was identifiable in *TaERF_1 BL*, and the EBE lies 171 bp upstream the ATG (Fig. 2*B* and *SI Appendix*, Fig. S3*B*).

Xtu strains occur as 2 types: A short lesion or low virulence cohort, represented here by *Xtu* strains LW16, XT130, and XT5791, and a high virulence cohort, represented by XT4699,

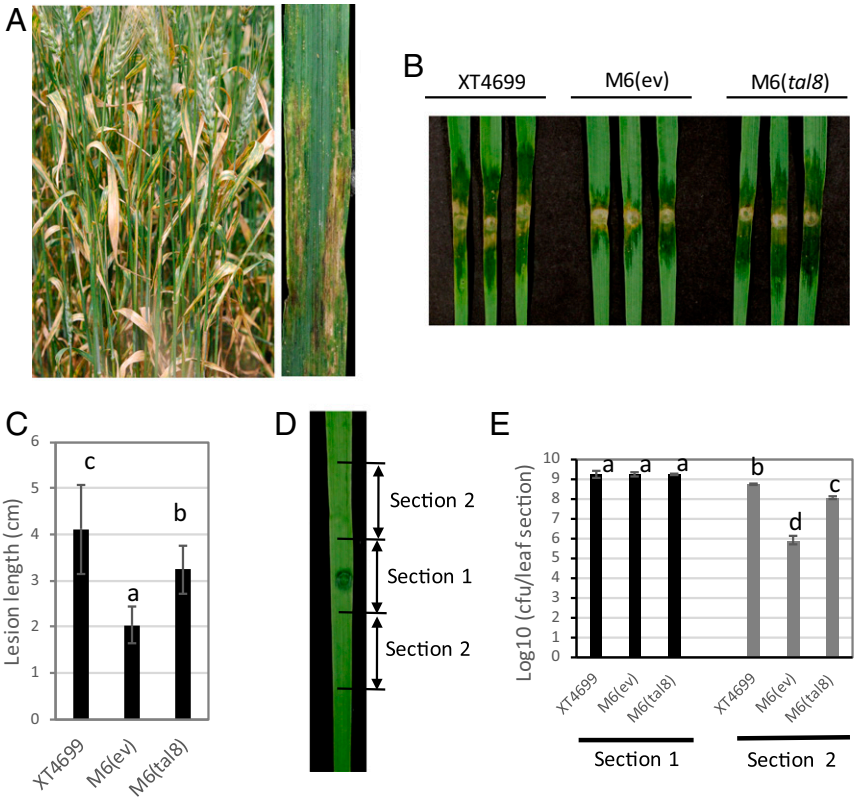

Fig. 1. Tal8 is associated with enhanced virulence. (*A*, *Left*) Field bacterial leaf streak infection of wheat. (*Right*) Individual leaf symptoms of infected leaf. (*B*) Photograph of representative leaves inoculated with bacterial strains with and without *tal8* at 7 d postinfection (DPI). XT4699, WT *Xtu*; M6(ev), *tal8*-deficient M6 strain harboring the empty vector pHM1; M6(tal8), M6 strain carrying *tal8* in pHM1. (*C*) Average lesion length measurements of 10 leaves at 5 DPI. Strains are as indicated in *B*. Each bar signifies the range of mean ± SD. The lowercase letters show significantly different groups ($P < 0.05$) using Tukey's honestly significant difference test (Tukey's HSD). (*D*) Schematic of bacterial leaf population measurements in sections at 7 DPI. Section 1 included the initial inoculation site and water-soaked tissue caused by M6(ev). Section 2 had an equal length to section 1. (*E*) Populations of bacteria in sections 1 and 2 as described in *D*. The lowercase letters indicate significantly different groups ($P < 0.05$) with Tukey's HSD.

Table 1. Candidate genes targeted by Tal8

	Gene ID	Gene name	EBE score*	Base pairs from ATG	Log_2FC in JA	Log_2FC in CS	Gene description
1	Traes_5BS_B626C522B	*TaNCED_5BS*	8	217	7.31	6.73	9-*cis*-epoxycarotenoid dioxygenase 3
2	Traes_7AS_25F9FEF52		8.91	467	4.45	1.91	Pyruvate dehydrogenase E1 component subunit α-2
3	Traes_1BL_F0C52C5DF	*TaERF_1BL*	9.02	171	6.50	7.01	AP2-like ethylene-responsive transcription factor
4	Traes_1AL_DEF14D73D	*TaERF_1AL*	9.02	NA	4.12	4.58	AP2-like ethylene-responsive transcription factor
5	Traes_1DL_E26B7E281	*TaERF_1DL*	9.02	181	3.82	3.78	AP2-like ethylene-responsive transcription factor
6	Traes_1AL_1B67D1299		9.11	388	4.25	2.42	Unknown protein
7	Traes_5DL_3A49B7207		9.4	118	3.09	0.20	Heat shock protein 21
8	Traes_4DS_033958E87		10.04	220	3.50	2.82	Early nodulin-like protein 22
9	Traes_2BL_172F729A7		10.57	356	3.44	2.07	Aluminum-induced protein with YGL and LRDR motifs
10	Traes_5DS_E58EBABFD	*TaNCED_5DS*	11	219	4.91	5.14	9-*cis*-epoxycarotenoid dioxygenase 3
11	Traes_1BL_6B21370DA		11.21	225	3.34	2.47	Eukaryotic peptide chain release factor subunits 1 and 2
12	Traes_2AL_B7FC2C090		11.47	261	3.39	2.86	Aluminum-induced protein with YGL and LRDR motifs
13	Traes_1DL_E331E6071		11.92	147	4.38	2.41	Protein kinase superfamily protein
14	Traes_1AL_61464BAA6		11.98	285	3.35	2.64	Unknown protein

CS, wheat cv. Chinese Spring; Log_2FC, the log_2 value of fold-change of WT vs. M6; JA, wheat cv.Jagger; NA, missed information of translation start codon in annotation.

*EBE score value is calculated by the target finder with best possible score of 4.9 for Tal8.

LG48, XT5523, XT5770, LB10, and P3 (Fig. 2*C*). Low and high expression levels of *TaNCED* and *TaERF* were associated with low and high virulence strains, respectively (Fig. 2*D*; primers used in this study are listed in *SI Appendix*, Table S2). Transfer of *tal8* into the low virulence strain LW16 resulted in a strain with greater virulence (Fig. 2 *E* and *F*) and enhanced expression of *TaNCED* and *TaERF* (Fig. 2*G*). Sequence analysis of representative low virulence strain LW16 and the high virulence strain P3 revealed that the chromosomes are colinear and contain 8 TAL effector genes in the same locations as XT4699 (*SI Appendix*, Fig. S4) (25, 26). The TAL effector genes of the 3 strains encode near-identical RVD repeats, with the exception that Tal8 of LW16, where the RVDs are highly dissimilar from XT4699 and P3 (*SI Appendix*, Fig. S5 and Table S3).

***TaNCED* Induction Contributes to High Virulence.** Designer TAL effectors (dTALes) were constructed to target unique sequences in the *TaNCED_5BS* and *TaERF_1BL* promoters, respectively, in order to induce each gene independently (*SI Appendix*). The dTALe dNCED72 targeted the EBE for Tal8 plus 3 additional nucleotides, while 3 other dTALes (dNCED41, dNCED53, and dNCED63) targeted the TATA box region downstream of the Tal8 EBE (Fig. 3*A*). Three dTALes—dERF3, dERF4, and dERF6—targeted the promoter region of *TaERF_1BL* upstream of the original Tal8 EBE (Fig. 3*B*). The dTALes were introduced individually into the Tal8-deficient low virulence strain LW16, which was used due to the higher natural competency for DNA transfer, and the strains were tested for the ability to promote expression of *TaNCED_5BS* and *TaERF_1BL*, respectively. The dTALe dNCED72 triggered the highest expression of *TaNCED_5BS* (Fig. 3*C*). However, dNCED72 also resulted in *TaERF_1BL* expression and, therefore, did not discriminate between the 2 genes (Fig. 3*C*). The dTALes dNCED41, dNCED53, and dNCED63 directed expression of *TaNCED_5BS* without concomitant expression of *TaERF_1BL* (Fig. 3*C*), and the dTALes dERF3, dERF4, and dERF6 each induced high levels of *TaERF_1BL* without *TaNCED_5BS* induction (Fig. 3*D*). Expression levels were so high for the ERF dTALes that we were concerned the high levels might have pleiotropic effects on the host physiology and, as a consequence, disease symptom expression. As an added caution, dERF101 was designed by the introduction of 4 RVDs with suboptimal matches with the corresponding nucleotides in the EBE for dERF3. LW16 carrying the dERF101 had lower induction on *TaERF_1BL*, although induction was higher in comparison to Tal8 (Fig. 3*D*). Upon inoculation of the strains with the dTALes on wheat, transformants carrying dTALes dNCED41, dNCED53, dNCED63, or dNCED72 enhanced virulence (Fig. 3*E*). Transformants harboring dERF3, dERF4, dERF6, or dERF101, targeting *TaERF_1BL* alone, did not promote virulence (Fig. 3*E*). The dTALes were also tested in the original *tal8* mutant strain M6 with similar results. The dTALes for *TaERF_1BL* and *TaNCED_5BS* induced the respective target genes, while only dNCED63 enhanced virulence based on lesion length (*SI Appendix*, Fig. S6). Therefore, pathogen virulence, in both LW16 and XT4699 and, conversely, host susceptibility are associated with NCED expression but not ERF expression.

Tal8 Directs Expression in Tobacco. *Agrobacterium*-mediated transient expression assays on *Nicotiana benthamiana* leaves were used to corroborate Tal8-directed expression specifically from the *TaNCED_5BS* and *TaNCED_5DS* promoters (*SI Appendix*). When fused with the reporter gene *uidA* for β-glucuronidase (GUS), the native promoters of *TaNCED_5BS* and *TaNCED_5DS* resulted in low GUS activity when coexpressed with Tal8 under the control of the CaMV 35S promoter, although the *TaNCED_5BS* promoter gave higher expression levels than *TaNCED_5DS* (Fig. 3*F*, $Tal8{+}NCED_B$ and $Tal8\_NCED_D$, respectively). As the wheat promoters may not function efficiently in *N. benthamiana*, the Tal8 EBEs for *TaNCED_5BS* and *TaNCED_5DS* were embedded in a truncated promoter for *CsLob1* (CsLobT) from citrus, which is

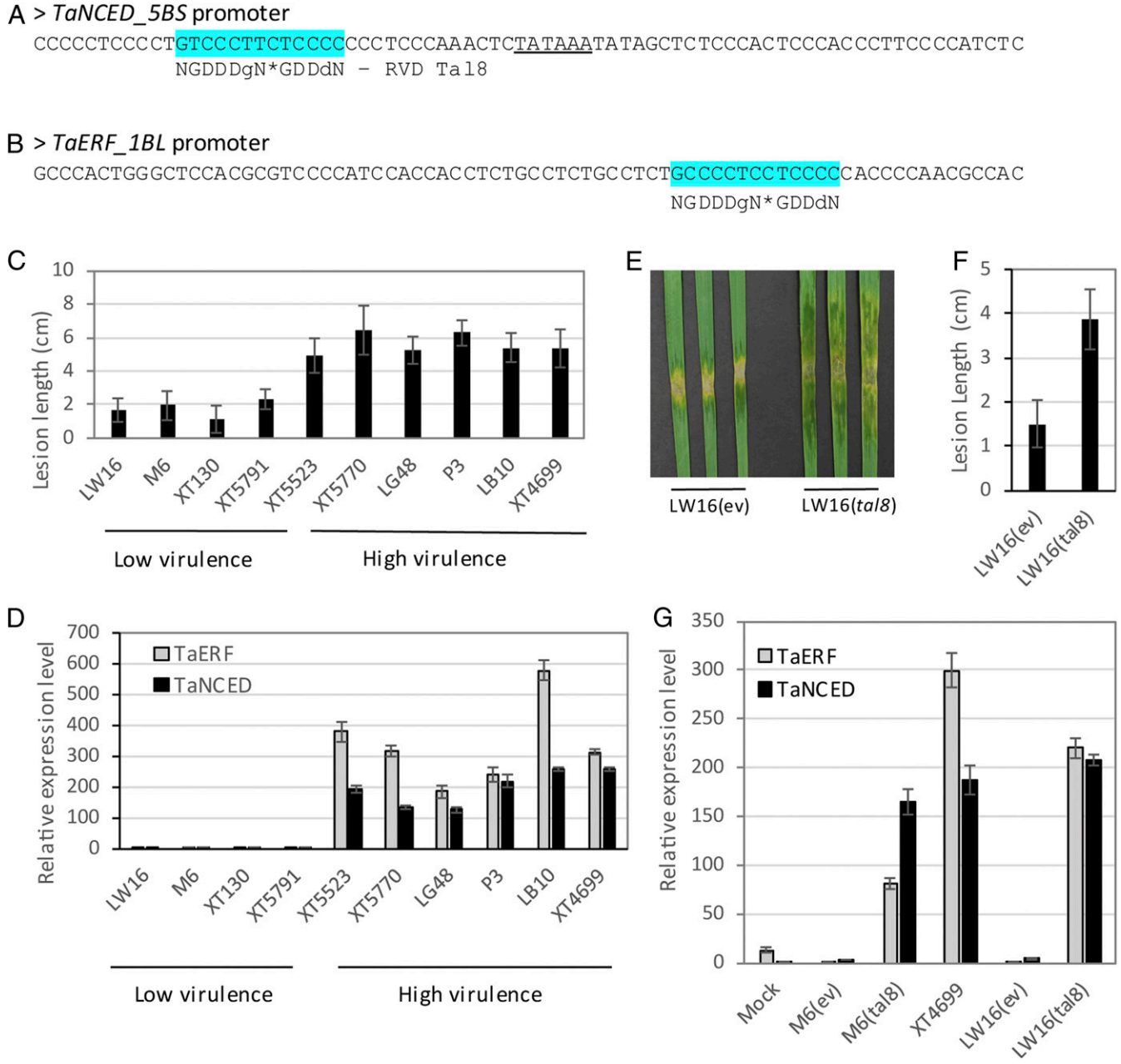

Fig. 2. *TaNCED_5BS* and *TaERF_1BL* expression is associated with virulence. (*A* and *B*) The alignments of predicted EBE (highlighted in turquoise) in the promoters of *TaNCED_5BS* and *TaERF_1BL*, respectively, with the RVDs of Tal8. (*C*) Lesion length measurements of low and high virulence strains of *Xtu*. (*D*) Expression levels of *TaNCED_5BS* and *TaERF_1BL* in low and high virulence strains of *Xtu*. (*E*) Introduction of *tal8* enhanced the lesion expansion for the low virulence strain LW16. LW16(ev), LW16 with empty vector pHM1; LW16(tal8), LW16 with *tal8* in pHM1. (*F*) The lesion length measurements after 7 DPI with LW16(ev) and LW16(tal8). (*G*) Expression levels of *TaNCED_5BS* and *TaERF_1BL* for M6 and LW16 strains with and without *tal8*. Mock, water inoculation. Leaves infiltrated with bacterial inoculum (OD_{600nm} = 0.2) were sampled at 1 DPI for all qRT-PCR assays.

efficiently expressed in tobacco (27). *CsLob1* and the derivative CsLobT contain the EBE for the TAL effector PthA4. CsLobT directed expression only when containing the Tal8 EBE from *TaNCED_5BS* or *TaNCED_5DS* and cotransformed with CaMV 35S regulated Tal8 or, as a control, CaMV 35S regulated PthA4 (Fig. 3*F*, Tal8+CsLobT, Tal8+EBE_B-CsLobT, Tal8+EBE_D-CsLobT, and PthA4+CsLobT, respectively). Again, the EBE from *TaNCED_5BS* (EBE_B) functioned better than the EBE from *TaNCED_5DS* (EBE_D) in the context of CsLobT, which is consistent with the RNA-seq data. GUS activity was undetectable with the promoter constructs EBE_B-CsLobT and EBE_D-CsLobT in the absence of Tal8 (Fig. 3*F*, ev+EBE_B-CsLobT and ev+EBE_D-CsLobT, respectively). The results corroborate the hypothesis that EBE_B and EBE_D mediate Tal8-associated expression of *TaNCED_5BS* (and *TaNCED_5DS*).

Increased ABA Content Is Associated with Virulence. NCED activity is the first committed step in the biosynthetic pathway for ABA, and 3 predicted products from the wheat genes on the short arm of chromosome 5 are most closely related to *OsNCED5* and *OsNCED3* of rice and *ZmVP14* of maize, 2 of which have been shown to be involved in ABA biosynthesis (*SI Appendix*, Fig. S7*A*) (28, 29). Indeed, the ABA content rose in infected leaf tissues upon NCED expression as measured by a competitive

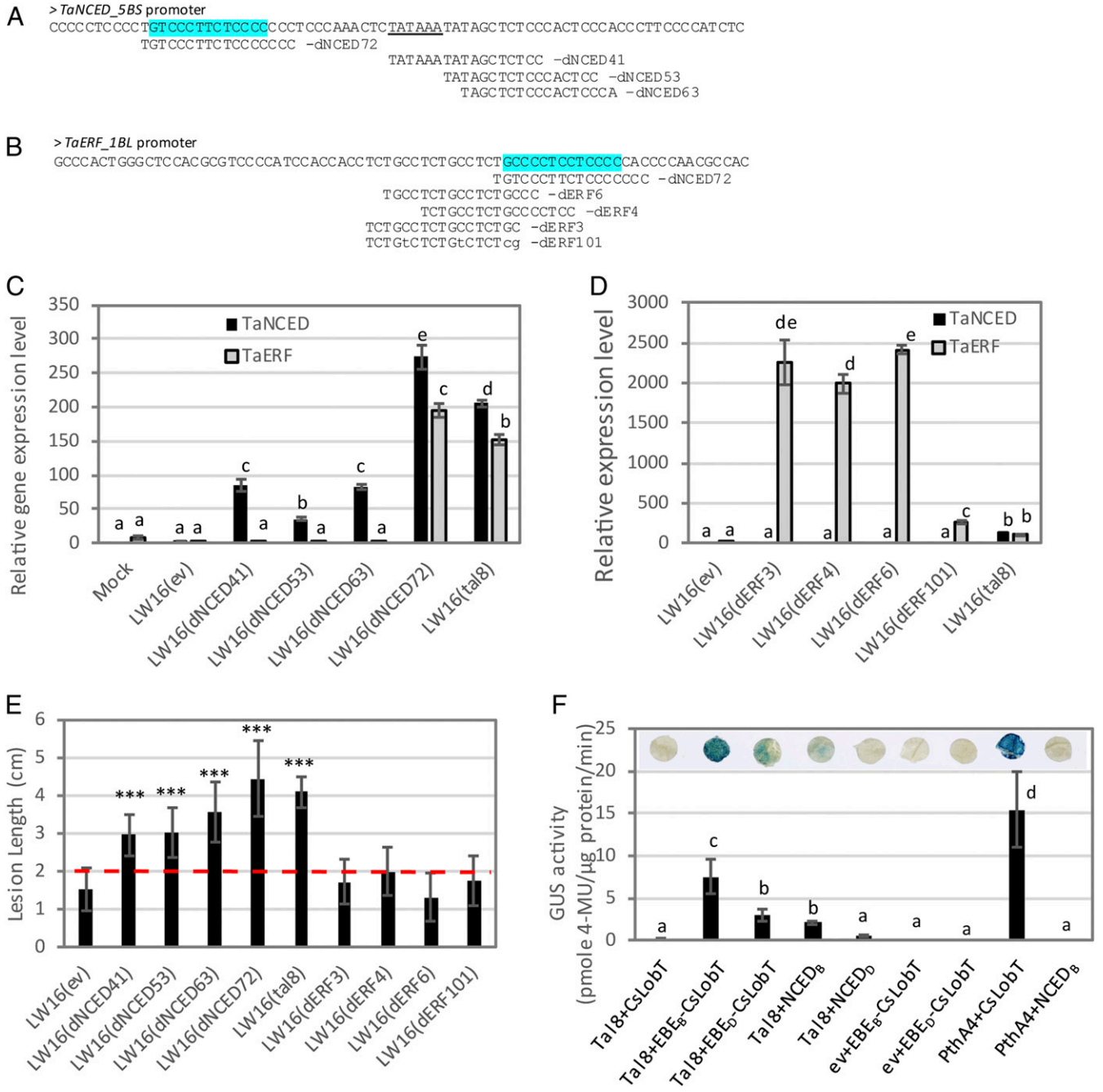

Fig. 3. *TaNCED_5BS* expression is correlated with enhanced virulence. (*A*) Four dTALes (dNCED41, dNCED53, dNCED63, and dNCED72) designed for the promoter region of *TaNCED_5BS*. (*B*) Four dTALes (dERF3, dERF4, dERF6, and dERF101) designed for the promoter region of *TaERF_1BL*. dERF101 were specifically designed with 4 fewer optimal matches, shown in lowercase letters, for reducing gene expression level. (*C*) Expression of *TaNCED_5BS* and not *TaERF_1BL* as measured by qRT-PCR by dNCED41, dNCED53, and dNCED63, while dNCED72 and Tal8 triggered expression of both genes. (*D*) Relative expression of *TaERF_1BL* based on qRT-PCR by dERF3, dERF4, dERF6, and dERF101. The lowercase letters indicate significantly different groups ($P < 0.05$) in the Tukey statistic and ANOVA analysis. (*E*) Lesion length measurements at 7 DPI with LW16 strains harboring dTALes, *tal8*, or empty vector (ev). ***$P < 0.001$, significant difference relative to lesion lengths of LW16(ev) (red dashed line) with Dunnett's multiple comparisons test and ANOVA analysis. (*F*) The EBE in the *TaNCED_5BS* directs Tal8-dependent transient GUS expression in *N. benthamiana*. Photographs of representative leaf disks are shown above each column stained with X-Gluc. The values indicate means ± SD ($n = 4$). Values with the same lowercase letters do not differ significantly ($P < 0.05$) by Tukey statistic and ANOVA analysis. Details about the *Agrobacterium*-mediated transient expression are described in *SI Appendix*.

ELISA (*SI Appendix*). Mock inoculations or inoculations with LW16 (ev), which does not induce the expression of *TaNCED_5BS*, were associated with low amounts of ABA in leaves (Fig. 4*A*). LW16 carrying dERF4 and dERF6 also did not enhance the ABA levels (Fig. 4*A*). Inoculations with LW16, containing dNCED41, dNCED53, dNCED63, dNCED72, or *tal8*, had high ABA levels (Fig. 4*A*). To determine if ABA was consequential to virulence, ABA was applied to leaves, which were challenged by low virulence pathogen. ABA application followed by LW16 (ev) inoculation resulted in 7-fold increase in lesion length along the leaf blade (Fig. 4 *B* and *C*) and higher bacterial populations in distal sections of the leaves in comparison to the control treatment without ABA (Fig. 4*D*, section 2).

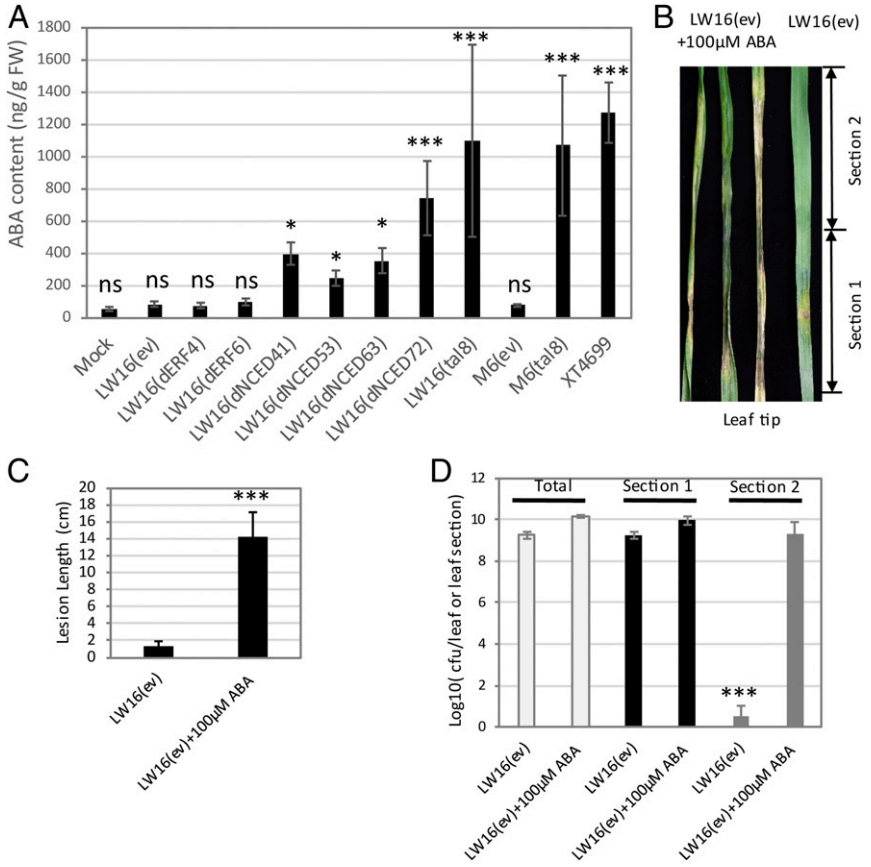

Fig. 4. Enhanced virulence is associated with elevated levels of ABA. (*A*) ABA levels in inoculated and control wheat leaves at 1 DPI with the indicated strains. The values showed the means ± SD. Significant difference was indicated above the column of ABA content of each sample with *P* value (**P* < 0.05; ****P* < 0.001) relative to ABA content of LW16(ev) treatment by Dunnett's multiple comparisons test and ANOVA analysis. The nonsignificant differences in the same statistical analysis are designated by "ns." (*B*) Photograph of wheat leaves after inoculation with LW16(ev) with and without exogenous ABA treatment at 7 DPI. Sections indicate regions selected for population measurements as presented below. (*C*) Lesion length measurements of LW16(ev) inoculated leaves sprayed with or without ABA. ****P* < 0.001, significant difference relative to lesion lengths of LW16(ev) without ABA spray in Student's *t* test. (*D*) Bacterial population of LW16(ev) in whole leaf or leaf sections (6 cm). Leaf sections were defined as in *B*. ****P* < 0.001, significant difference between the 2 values in section 2 with Student's *t* test.

Tal8 and ABA Alter Water Relations in the Host. Plant pathogenic bacteria are hypothesized to engineer a favorable aqueous intercellular environment in the host (30–32). ABA, as the classic hormone in response to water-stress, might be hijacked to recruit and retain water at the site of infection. ABA induces stomatal closure and consequential reductions of gas and water transpiration. Indeed, transpiration, as well as water loss, were reduced in tissues infected with bacteria containing Tal8 (Fig. 5 *A* and *B*). Water-soaked lesions are thought to reflect release of water from mesophyll cells into the intercellular space (apoplast) upon infection. Here, we observed that ABA application by itself promoted water-soaking symptoms, indicating that the retention of water to the site of infection may also occur (Fig. 5*C*). HopAM1 of *P. syringae* was reported to be effective in water-stressed plants (18). Here, the plants were tested under well-watered conditions. However, inoculation of plants under high humidity enhanced lesion lengths and reduced the differences between strains with and without Tal8 (Fig. 5*D*), indicating the reduced water loss under higher humidity enhances disease and bacterial spread.

Tal8 Is Associated with Reduced Expression of *TaNPR1*. ABA-mediated disease susceptibility has been hypothesized to be due to antagonism to the salicylic acid (SA) defense response (33–36). SA levels were measured over a 3-d period after infection. SA levels, both free and total, rose over a 3-d period after infection of wheat leaves with LW16 (ev), LW16(dNCED63), and LW16 (*tal8*) (*SI Appendix*, Fig. S7 *B* and *C*). Free SA levels between the strains with and without *tal8* rose to similar levels (*SI Appendix*, Fig. S7*B*). Total SA levels were also higher over the same period (*SI Appendix*, Fig. S7*C*). LW16(dNCED63) had the highest free and total SA (*SI Appendix*, Fig. S7 *B* and *C*), although this strain, similar to the strain with *tal8*, also has enhanced lesion lengths and ABA content. Therefore, SA content did not vary strictly in relation to TaNCED expression. Application of SA, both by leaf spray or soil drench, did not alter susceptibility of LW16 with or without *tal8* (*SI Appendix*, Fig. S7 *D* and *E*). Nonetheless, changes in expression of wheat homologs of the master immune regulator and SA receptor gene *TaNPR1* were observed in infected tissues by strains with or without *tal8*. Both A and D genome copies of the gene were lower in expression in the presence of Tal8 (Fig. 6*A*). *TaNPR1* suppression was correlated with NCED expression as a strain with dTALe targeting TaNCED (dNCED63) also suppressed NPR1 based on the expression of *TaNPR1_3AS*, while the strain with dERF101 failed to suppress (Fig. 6*B*). Leaf infiltration of ABA resulted in the largest suppression *TaNPR1* (Fig. 6*B*). Reduced NPR1 expression was correlated with reduced expression of homologs of the NPR1-dependent defense gene *PR1* (Fig. 6 *C* and *D*). SA levels, then, may be less relevant than NPR1 levels due to suppression of NPR1 expression by ABA.

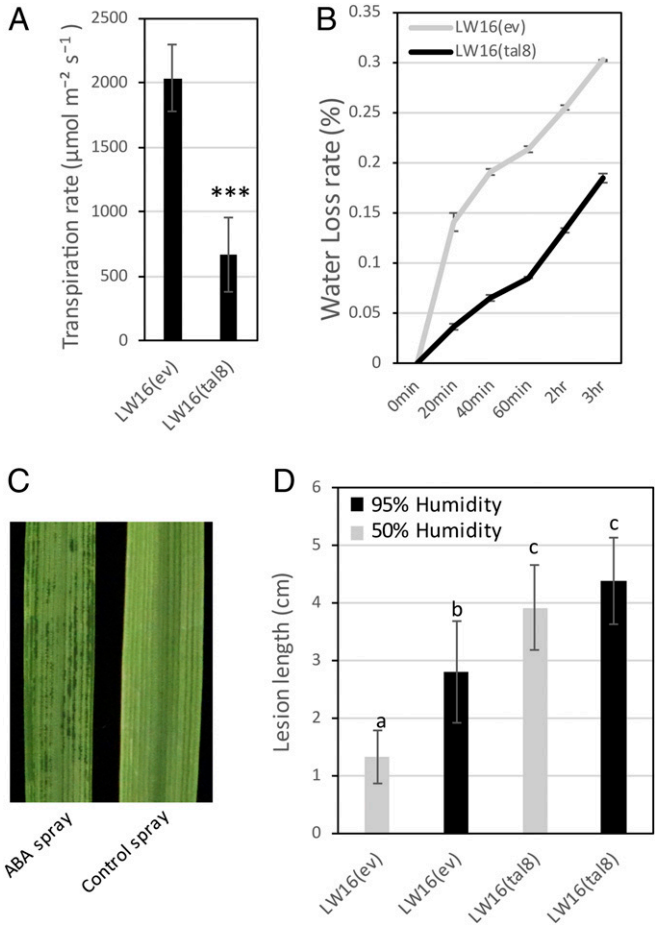

Fig. 5. ABA effects on leaf physiology. (*A*) Transpiration rate was reduced in leaves infiltrated with LW16(*tal8*) in comparison to LW16(ev) at 1 DPI. Bacterial suspensions (OD_{600nm} = 0.2) were applied. ***$P < 0.001$, significant difference between the 2 values with Student's *t* test. (*B*) Water loss was inhibited in detached leaves infiltrated with LW16(*tal8*) compared to leaves inoculated by LW16(ev) at 1 DPI with bacterial inoculum (OD_{600nm} = 0.2). (*C*) The water-soaked leaves photographed 1 d after spraying with ABA (100 μM) in 0.02% Silwet L–77. (*D*) Lesion length measurement of bacterial inoculations (OD_{600nm} = 0.2) under high humidity (95%) and control humidity (50%) at 7 DPI. The lowercase letters indicate significantly different groups ($P < 0.05$) by Tukey's HSD.

Discussion

Plant-associated bacteria have multiple demonstrated mechanisms to alter the phytohormone content of the host. Here, we show that *Xtu* has adapted to wheat by targeting a susceptibility gene, *TaNCED*, principally the gene *TaNCED_5BS* on the short arm of chromosome 5B of hexaploid wheat, accessing phytohormone production directly through ectopic induction of otherwise regulated host pathways. We propose that the TAL effector Tal8 directly stimulates the pathway for ABA, mediated by interaction at the EBE in the promoters of *TaNCED_5BS* and *TaNCED_5DS* and, furthermore, that ABA enhances disease susceptibility. Promoter sequence similarities between *TaNCED_5BS* and *TaERF_1BL* result in the induction of both genes by Tal8, and the possibility exists that the similarities reflect coregulation and interaction in normal plants. ABA insensitive 4 (AIB4) and multiple drought-responsive element binding factors, which mediate control of many ABA responsive elements, are members of the AP2/ERF transcription factor family (37), and enhanced expression of 1 or more of these genes might act synergistically with ABA to enhance susceptibility. However, under the conditions used here, no evidence could be found for involvement of *TaERF_1BL* in virulence, independent of NCED expression. The candidate EBEs in both NCED genes directed expression in a Tal8-mediated manner in a transient expression system, and polymorphisms between the EBEs are reflected in differing levels of expression in vivo and in the transient expression system. Nonetheless, future genome editing of the EBEs will provide important corroborative evidence that the EBEs, indeed, are the critical Tal8 binding site.

The benefits of Tal8 and consequential high ABA levels could be due to multiple factors. The effects of ABA on disease susceptibility has been attributed to 3 possible factors, which are not mutually exclusive: Suppression of SA pathway defense responses, inactivation of defense-related MAP kinases, and alteration of water availability at the infection site (17, 18, 33). The effects of humidity on lesion development and reduction of the differences between bacteria with and without Tal8 corroborates the importance of water relations. Rice mutants, for example, with severely reduced ABA levels, are resistant to infection by *X*anthomonas *oryzae* pv. *oryzae*, the agent of bacterial blight of rice, and reductions in stomatal conductance, water transpiration, and higher ABA content accompany bacterial blight infections of normal plants (38). In the latter study, no evidence could be found to support an alteration in SA signaling in contrast to 2 other studies of ABA content in disease susceptibility (34, 36). We found variable changes in free and total SA content of infected wheat leaves in association with TALe-mediated ABA increases and could not discern a firm contribution to disease susceptibility. At the same time, some contribution of SA cannot be ruled out. *NPR1* plays essential roles in localized and systemic acquired resistance in many plant species and overexpression of *NPR1* in wheat enhances disease resistance (39, 40). Reduced expression of *TaNPR1*, which is involved in SA perception, was observed and, coincidently, is a unique finding for an effector function. These data indicate that ABA production induced by Tal8 may impact susceptibility to *Xtu* by suppressing the ability of the plant to perceive SA. Similar antagonistic relationships between ABA and NPR1 have been observed in other plant species, for example NPR1 protein degradation is stimulated by ABA in *Arabidopsis* (41). Suppression of NPR1 expression by ABA has also been observed in rice (35, 36), indicating that ABA-mediated regulation of *NPR1* maybe a conserved function of ABA in phytohormone cross-talk. The effects of Tal8 or ABA, directly, on MPK6 and MPK3 phosphorylation were not measured for *Xtu* infections, but inactivation of the defense-related kinases, as observed previously in *Arabidopsis*, may also contribute to enhance susceptibility of the host (17).

The enhancement of ABA levels by the TAL effector directed expression of NCED joins a growing list of TAL effector-mediated changes in host susceptibility. Rice is essentially immune to bacterial blight, if not for TAL effector-mediated induction of 1 of the SWEET gene family by strains of *X. oryzae* pv. *oryzae*, the products of which transport sucrose and, by an unknown mechanism, enhance host susceptibility (42). SWEET gene induction also occurs in bacterial angular spot disease of cotton and bacterial blight of cassava (43, 44). The benefits of SWEET gene expression have been attributed to the elevated access to sugar as a nutrient for pathogen growth (45). Three host transcription factor genes are known to be targeted in diseases of pepper, citrus, and tomato (27, 31, 46). The latter 2 cases are associated with coexpression of cell wall degradative enzymes, which may release of bacteria from the infection site or alter water content of the infected tissue (31). In the case of *Xtu*, increased release of bacteria from the leaf surface was not detected. Nonetheless, bacteria were found to spread farther up and down the leaf in the presence of NCED expression. The spread could be driven by water flow into the infected area due to stomatal closure, enhanced bacterial growth by a more aqueous environment, or a combination of ABA effects. A variety of additional TAL effector host targets are associated with virulence effects (47–49). TAL effectors, therefore, represent a

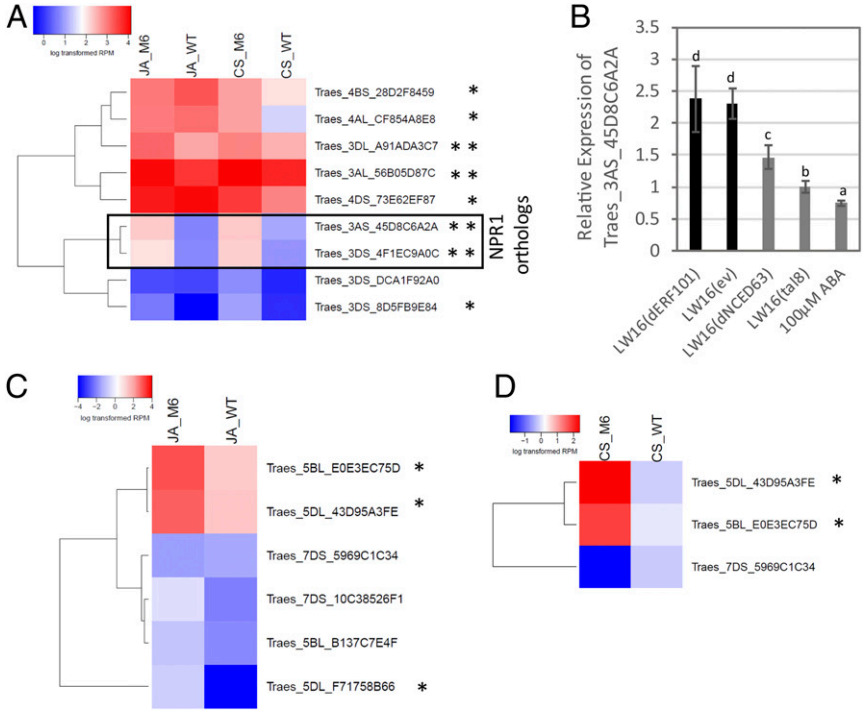

Fig. 6. Tal8 effector suppresses expression of *NPR1* and *PR1* in wheat. (*A*) Heatmap of *TaNPR1* expression in 2 wheat cultivars after inoculation with the mutant (M6) or the WT strain XT4699. One and 2 asterisks indicate significant difference in the Chinese Spring (CS) comparison and in both Jagger (JA) and Chinese Spring (CS) comparisons, respectively (q value < 0.05). The boxed area indicates 2 predicted orthologs of *NPRI* in wheat. RPM represents reads per million of total reads. (*B*) Expression quantification by qRT-PCR of Traes_3AS_45D8C6A2A in cv. Jagger. The leaves infiltrated with bacterial inoculum at (OD_{600nm} = 0.2) or 100 μM ABA were sampled at 1 DPI. Different letters indicate statistical significantly different groups (P < 0.05) by Tukey's HSD. (*C*) Heatmap of *PR1* genes in comparison of inoculated wheat samples between M6 and WT in wheat cv. JA. Three genes were suppressed in WT *Xtu* treatment. (*D*) Expression of 2 wheat *PR1* genes was suppressed in cv. Chinese Spring (CS), respectively. The asterisk (*) indicates the significant difference under q value < 0.05.

versatile method to manipulate host susceptibility, and the list of TALe-mediated changes in plant physiological processes potentially affecting disease susceptibility is growing (50). The mechanisms by which known host S genes mediate enhanced virulence are poorly understood. Due to the extensive knowledge of ABA function, the consequences of Tal8 seem amenable for further elucidation.

Materials and Methods

The wheat plants were grown and inoculated for virulence assays in growth chambers with control conditions as described in *SI Appendix*. Bacteria and plasmids used in this study are provided in *SI Appendix*, Table S1. Methods on RNA-seq analyses, prediction of candidate S genes for Tal8 and heatmap constructions, and sequence analysis of additional low and high virulence strains of *Xtu* are provided in detail in *SI Appendix*. Repeats of dTALes were assembled following methods described previously (51, 52). dTALes were cloned into broad host-range vector pHM1 and transformed into *Xanthomonas* bacteria for functional tests. Further methods on qRT-PCR analyses, transient GUS assay in *N. benthamiana*, ABA quantification assay, application of ABA and effect of Tal8 in wheat leaves, and SA measurement and application are described in detail in *SI Appendix*.

ACKNOWLEDGMENTS. The authors thank Dr. Alina Akhunova and the staff of the Kansas Integrated Genomic Facility at Kansas State University for RNA sequencing; Dr. Matthew Dommel, and Dr. Zhonglin Mou for assistance with salicylic acid assays; and Dr. Sixue Chen and Mr. Oijie Guan for assistance with leaf transpiration measurements. This research was supported by funds from the National Science Foundation research Grants 1238189 (to F.F.W.) and 1741090 (to S.L., S.P., and F.F.W.), and the Institute of Food and Agricultural Sciences, University of Florida (F.F.W.).

1. A. Robert-Seilaniantz, M. Grant, J. D. Jones, Hormone crosstalk in plant disease and defense: More than just jasmonate-salicylate antagonism. *Annu. Rev. Phytopathol.* **49**, 317–343 (2011).
2. K. Kazan, R. Lyons, Intervention of phytohormone pathways by pathogen effectors. *Plant Cell* **26**, 2285–2309 (2014).
3. E. Stes *et al*., The leafy gall syndrome induced by *Rhodococcus fascians*. *FEMS Microbiol. Lett.* **342**, 187–194 (2013).
4. R. Nagel, R. J. Peters, Investigating the phylogenetic range of gibberellin biosynthesis in bacteria. *Mol. Plant Microbe Interact.* **30**, 343–349 (2017).
5. M. Cerboneschi *et al*., Indole-3-acetic acid in plant-pathogen interactions: A key molecule for in planta bacterial virulence and fitness. *Res. Microbiol.* **167**, 774–787 (2016).
6. S. A. McClerklin *et al*., Indole-3-acetaldehyde dehydrogenase-dependent auxin synthesis contributes to virulence of *Pseudomonas syringae* strain DC3000. *PLoS Pathog.* **14**, e1006811 (2018).
7. D. E. Akiyoshi, H. Klee, R. M. Amasino, E. W. Nester, M. P. Gordon, T-DNA of *Agrobacterium tumefaciens* encodes an enzyme of cytokinin biosynthesis. *Proc. Natl. Acad. Sci. U.S.A.* **81**, 5994–5998 (1984).
8. M. F. Thomashow, S. Hugly, W. G. Buchholz, L. S. Thomashow, Molecular basis for the auxin-independent phenotype of crown gall tumor tissues. *Science* **231**, 616–618 (1986).
9. B. Thines *et al*., JAZ repressor proteins are targets of the SCF(COI1) complex during jasmonate signalling. *Nature* **448**, 661–665 (2007).
10. F. Cui *et al*., The *Pseudomonas syringae* type III effector AvrRpt2 promotes pathogen virulence via stimulating Arabidopsis auxin/indole acetic acid protein turnover. *Plant Physiol.* **162**, 1018–1029 (2013).
11. S. Jiang *et al*., Bacterial effector activates jasmonate signaling by directly targeting JAZ transcriptional repressors. *PLoS Pathog.* **9**, e1003715 (2013).
12. S. Gimenez-Ibanez *et al*., The bacterial effector HopX1 targets JAZ transcriptional repressors to activate jasmonate signaling and promote infection in *Arabidopsis*. *PLoS Biol.* **12**, e1001792 (2014).
13. X. Han, R. Kahmann, Manipulation of phytohormone pathways by effectors of filamentous plant pathogens. *Front. Plant Sci.* **10**, 822 (2019).
14. M. F. Pye, S. M. Dye, R. S. Resende, J. D. MacDonald, R. M. Bostock, Abscisic acid as a dominant signal in tomato during salt stress predisposition to phytophthora root and crown rot. *Front. Plant Sci.* **9**, 525 (2018).
15. Y. P. Ho *et al*., The AvrB_AvrC domain of AvrXccC of *Xanthomonas campestris* pv. *campestris* is required to elicit plant defense responses and manipulate ABA homeostasis. *Mol. Plant Microbe Interact.* **26**, 419–430 (2013).
16. M. de Torres-Zabala *et al*., *Pseudomonas syringae* pv. tomato hijacks the *Arabidopsis* abscisic acid signalling pathway to cause disease. *EMBO J.* **26**, 1434–1443 (2007).

17. A. Mine *et al*., Pathogen exploitation of an abscisic acid- and jasmonate-inducible MAPK phosphatase and its interception by *Arabidopsis* immunity. *Proc. Natl. Acad. Sci. U.S.A.* **114**, 7456–7461 (2017).
18. A. K. Goel *et al*., The *Pseudomonas syringae* type III effector HopAM1 enhances virulence on water-stressed plants. *Mol. Plant Microbe Interact.* **21**, 361–370 (2008).
19. B. Yang, A. Sugio, F. F. White, *Os8N3* is a host disease-susceptibility gene for bacterial blight of rice. *Proc. Natl. Acad. Sci. U.S.A.* **103**, 10503–10508 (2006).
20. J. Boch, U. Bonas, *Xanthomonas* AvrBs3 family-type III effectors: Discovery and function. *Annu. Rev. Phytopathol.* **48**, 419–436 (2010).
21. M. J. Moscou, A. J. Bogdanove, A simple cipher governs DNA recognition by TAL effectors. *Science* **326**, 1501 (2009).
22. N. Falahi Charkhabi *et al*., Complete genome sequencing and targeted mutagenesis reveal virulence contributions of Tal2 and Tal4b of *Xanthomonas translucens* pv. *undulosa* ICMP11055 in bacterial leaf streak of wheat. *Front. Microbiol.* **8**, 1488 (2017).
23. Z. Peng *et al*., Long read and single molecule DNA sequencing simplifies genome assembly and TAL effector gene analysis of *Xanthomonas translucens*. *BMC Genomics* **17**, 21 (2016).
24. Y. Hu, Z. Peng, S. Liu, F. White, Xanthomonas translucens directly induces abscisic acid biosynthesis to enhance disease susceptibility in wheat. Sequence Read Archive. https://www.ncbi.nlm.nih.gov/bioproject/PRJNA485724. Deposited 13 August 2018.
25. Z. Peng, J. C. Huguet-Tapia, F. F. White, Xanthomonas translucens pv. undulosa strain LW16 chromosome. GenBank. https://www.ncbi.nlm.nih.gov/nuccore/CP043540.1/. Deposited 31 August 2019.
26. Z. Peng, J. C. Huguet-Tapia, F. F. White, Xanthomonas translucens pv. undulosa strain P3 chromosome. GenBank. https://www.ncbi.nlm.nih.gov/nuccore/CP043500/. Deposited 31 August 2019.
27. Y. Hu *et al*., *Lateral organ boundaries 1* is a disease susceptibility gene for citrus bacterial canker disease. *Proc. Natl. Acad. Sci. U.S.A.* **111**, E521–E529 (2014).
28. S.-G. Hwang *et al*., Ectopic expression of rice *OsNCED3* in Arabidopsis increases ABA level and alters leaf morphology. *Plant Sci.* **178**, 12–22 (2010).
29. S. H. Schwartz, B. C. Tan, D. A. Gage, J. A. Zeevaart, D. R. McCarty, Specific oxidative cleavage of carotenoids by VP14 of maize. *Science* **276**, 1872–1874 (1997).
30. G. A. Beattie, Water relations in the interaction of foliar bacterial pathogens with plants. *Annu. Rev. Phytopathol.* **49**, 533–555 (2011).
31. A. R. Schwartz, R. Morbitzer, T. Lahaye, B. J. Staskawicz, TALE-induced bHLH transcription factors that activate a pectate lyase contribute to water soaking in bacterial spot of tomato. *Proc. Natl. Acad. Sci. U.S.A.* **114**, E897–E903 (2017).
32. X. F. Xin *et al*., Bacteria establish an aqueous living space in plants crucial for virulence. *Nature* **539**, 524–529 (2016).
33. M. de Torres Zabala, M. H. Bennett, W. H. Truman, M. R. Grant, Antagonism between salicylic and abscisic acid reflects early host-pathogen conflict and moulds plant defence responses. *Plant J.* **59**, 375–386 (2009).
34. K. Audenaert, G. B. De Meyer, M. M. Höfte, Abscisic acid determines basal susceptibility of tomato to *Botrytis cinerea* and suppresses salicylic acid-dependent signaling mechanisms. *Plant Physiol.* **128**, 491–501 (2002).
35. C. J. Jiang *et al*., Abscisic acid interacts antagonistically with salicylic acid signaling pathway in rice-*Magnaporthe grisea* interaction. *Mol. Plant Microbe Interact.* **23**, 791–798 (2010).
36. J. Xu, K. Audenaert, M. Hofte, D. De Vleesschauwer, Abscisic acid promotes susceptibility to the rice leaf blight pathogen *Xanthomonas oryzae* pv *oryzae* by suppressing salicylic acid-mediated defenses. *PLoS One* **8**, e67413 (2013).
37. J. Mizoi, K. Shinozaki, K. Yamaguchi-Shinozaki, AP2/ERF family transcription factors in plant abiotic stress responses. *Biochim. Biophys. Acta* **1819**, 86–96 (2012).
38. D. Zhang, C. Tian, K. Yin, W. Wang, J. L. Qiu, Post-invasive bacterial resistance conferred by open stomata in rice. *Mol. Plant Microbe Interact.* **32**, 255–266 (2018).
39. J. Withers, X. Dong, Posttranslational modifications of NPR1: A single protein playing multiple roles in plant immunity and physiology. *PLoS Pathog.* **12**, e1005707 (2016).
40. R. Makandar, J. S. Essig, M. A. Schapaugh, H. N. Trick, J. Shah, Genetically engineered resistance to Fusarium head blight in wheat by expression of *Arabidopsis* NPR1. *Mol. Plant Microbe Interact.* **19**, 123–129 (2006).
41. Y. Ding, M. Dommel, Z. Mou, Abscisic acid promotes proteasome-mediated degradation of the transcription coactivator NPR1 in *Arabidopsis thaliana*. *Plant J.* **86**, 20–34 (2016).
42. . M. Bezrutczyk *et al*., Sugar flux and signaling in plant-microbe interactions. *Plant J.* **93**, 675–685 (2018).
43. K. L. Cox *et al*., TAL effector driven induction of a SWEET gene confers susceptibility to bacterial blight of cotton. *Nat. Commun.* **8**, 15588 (2017).
44. M. Cohn *et al*., *Xanthomonas axonopodis* virulence is promoted by a transcription activator-like effector-mediated induction of a SWEET sugar transporter in cassava. *Mol. Plant Microbe Interact.* **27**, 1186–1198 (2014).
45. L. Q. Chen *et al*., Sugar transporters for intercellular exchange and nutrition of pathogens. *Nature* **468**, 527–532 (2010).
46. S. Kay, S. Hahn, E. Marois, G. Hause, U. Bonas, A bacterial effector acts as a plant transcription factor and induces a cell size regulator. *Science* **318**, 648–651 (2007).
47. R. A. Cernadas *et al*., Code-assisted discovery of TAL effector targets in bacterial leaf streak of rice reveals contrast with bacterial blight and a novel susceptibility gene. *PLoS Pathog.* **10**, e1003972 (2014).
48. A. Sugio, B. Yang, T. Zhu, F. F. White, Two type III effector genes of *Xanthomonas oryzae* pv. oryzae control the induction of the host genes *OsTFIIA*gamma1 and *OsTFX1* during bacterial blight of rice. *Proc. Natl. Acad. Sci. U.S.A.* **104**, 10720–10725 (2007).
49. T. T. Tran *et al*., Functional analysis of African *Xanthomonas oryzae* pv. oryzae TALomes reveals a new susceptibility gene in bacterial leaf blight of rice. *PLoS Pathog.* **14**, e1007092 (2018).
50. S. Mücke *et al*., Transcriptional reprogramming of rice cells by *Xanthomonas oryzae* TALEs. *Front. Plant Sci.* **10**, 162 (2019).
51. T. Cermak *et al*., Efficient design and assembly of custom TALEN and other TAL effector-based constructs for DNA targeting. *Nucleic Acids Res.* **39**, e82 (2011).
52. T. Li *et al*., Modularly assembled designer TAL effector nucleases for targeted gene knockout and gene replacement in eukaryotes. *Nucleic Acids Res.* **39**, 6315–6325 (2011).